EUROPEAN ORGANIZATION FOR NUCLEAR RESEARCH

CERN–PPE/97–141

22 October 1997

m_b at M_Z

DELPHI Collaboration

Abstract

The value of the b quark mass at the M_Z scale defined in the $\overline{MS}$ renormalization scheme, $m_b(M_Z)$, was determined using 2.8 million hadronic Z decays collected during 1992-1994 by the DELPHI detector to be

$$m_b(M_Z) = 2.67 \pm 0.25 \text{ (stat.)} \pm 0.34 \text{ (frag.)} \pm 0.27 \text{ (theo.) GeV/c}^2.$$

The analysis considers NLO corrections to the three-jet production rate including mass effects, and the result obtained agrees with the QCD prediction of having a running b quark mass at an energy scale equal to M_Z. This is the first time that such a measurement is performed far above the $b\overline{b}$ production threshold. The study also verifies the flavour independence of the strong coupling constant for b and light quarks within 1% accuracy.

(Accepted by Physics Letters B)

P.Abreu[21], W.Adam[49], T.Adye[36], P.Adzic[11], I.Ajinenko[41], G.D.Alekseev[16], R.Alemany[48], P.P.Allport[22], S.Almehed[24], U.Amaldi[9], S.Amato[46], P.Andersson[43], A.Andreazza[9], P.Antilogus[9], W-D.Apel[17], Y.Arnoud[14], B.Åsman[43], J-E.Augustin[25], A.Augustinus[9], P.Baillon[9], P.Bambade[19], F.Barao[21], M.Barbi[46], G.Barbiellini[45], D.Y.Bardin[16], G.Barker[9], A.Baroncelli[39], O.Barring[24], M.J.Bates[36], M.Battaglia[15], M.Baubillier[23], J.Baudot[38], K-H.Becks[51], M.Begalli[6], P.Beilliere[8], Yu.Belokopytov[9,52], K.Belous[41], A.C.Benvenuti[5], C.Berat[14], M.Berggren[46], D.Bertini[25], D.Bertrand[2], M.Besancon[38], F.Bianchi[44], M.Bigi[44], M.S.Bilenky[16], P.Billoir[23], M-A.Bizouard[19], D.Bloch[10], M.Blume[51], M.Bonesini[27], W.Bonivento[27], M.Boonekamp[38], P.S.L.Booth[22], A.W.Borgland[4], G.Borisov[38,41], C.Bosio[39], O.Botner[47], E.Boudinov[30], B.Bouquet[19], C.Bourdarios[19], T.J.V.Bowcock[22], I.Bozovic[11], M.Bozzo[13], P.Branchini[39], K.D.Brand[35], T.Brenke[51], R.A.Brenner[47], R.C.A.Brown[9], P.Bruckman[35], J-M.Brunet[8], L.Bugge[32], T.Buran[32], T.Burgsmueller[51], P.Buschmann[51], S.Cabrera[48], M.Caccia[27], M.Calvi[27], A.J.Camacho Rozas[40], T.Camporesi[9], V.Canale[37], M.Canepa[13], F.Carena[9], L.Carroll[22], C.Caso[13], M.V.Castillo Gimenez[48], A.Cattai[9], F.R.Cavallo[5], V.Chabaud[9], Ph.Charpentier[9], L.Chaussard[25], P.Checchia[35], G.A.Chelkov[16], M.Chen[2], R.Chierici[44], P.Chliapnikov[41], P.Chochula[7], V.Chorowicz[25], J.Chudoba[29], V.Cindro[42], P.Collins[9], M.Colomer[48], R.Contri[13], E.Cortina[48], G.Cosme[19], F.Cossutti[45], J-H.Cowell[22], H.B.Crawley[1], D.Crennell[36], G.Crosetti[13], J.Cuevas Maestro[33], S.Czellar[15], J.Dahm[51], B.Dalmagne[19], G.Damgaard[28], P.D.Dauncey[36], M.Davenport[9], W.Da Silva[23], A.Deghorain[2], G.Della Ricca[45], P.Delpierre[26], N.Demaria[34], A.De Angelis[9], W.De Boer[17], S.De Brabandere[2], C.De Clercq[2], C.De La Vaissiere[23], B.De Lotto[45], A.De Min[35], L.De Paula[46], H.Dijkstra[9], L.Di Ciaccio[37], A.Di Diodato[37], A.Djannati[8], J.Dolbeau[8], K.Doroba[50], M.Dracos[10], J.Drees[51], K.-A.Drees[51], M.Dris[31], J-D.Durand[25,9], D.Edsall[1], R.Ehret[17], G.Eigen[4], T.Ekelof[47], G.Ekspong[43], M.Ellert[47], M.Elsing[9], J-P.Engel[10], B.Erzen[42], M.Espirito Santo[21], E.Falk[24], G.Fanourakis[11], D.Fassouliotis[45], J.Fayot[23], M.Feindt[17], P.Ferrari[27], A.Ferrer[48], S.Fichet[23], A.Firestone[1], P.-A.Fischer[9], H.Foeth[9], E.Fokitis[31], F.Fontanelli[13], F.Formenti[9], B.Franek[36], A.G.Frodesen[4], R.Fruhwirth[49], F.Fulda-Quenzer[19], J.Fuster[48], A.Galloni[22], D.Gamba[44], M.Gandelman[46], C.Garcia[48], J.Garcia[40], C.Gaspar[9], U.Gasparini[35], Ph.Gavillet[9], E.N.Gazis[31], D.Gele[10], J-P.Gerber[10], L.Gerdyukov[41], R.Gokieli[50], B.Golob[42], P.Goncalves[21], G.Gopal[36], L.Gorn[1], M.Gorski[50], Yu.Gouz[44,52], V.Gracco[13], E.Graziani[39], C.Green[22], A.Grefrath[51], P.Gris[38], G.Grosdidier[19], K.Grzelak[50], M.Gunther[47], J.Guy[36], F.Hahn[9], S.Hahn[51], S.Haider[9], Z.Hajduk[18], A.Hallgren[47], K.Hamacher[51], F.J.Harris[34], V.Hedberg[24], S.Heising[17], R.Henriques[21], J.J.Hernandez[48], P.Herquet[2], H.Herr[9], T.L.Hessing[34], J.-M.Heuser[51], E.Higon[48], S-O.Holmgren[43], P.J.Holt[34], D.Holthuizen[30], S.Hoorelbeke[2], M.Houlden[22], J.Hrubec[49], K.Huet[2], K.Hultqvist[43], J.N.Jackson[22], R.Jacobsson[43], P.Jalocha[9], R.Janik[7], Ch.Jarlskog[24], G.Jarlskog[24], P.Jarry[38], B.Jean-Marie[19], E.K.Johansson[43], L.Jonsson[24], P.Jonsson[24], C.Joram[9], P.Juillot[10], M.Kaiser[17], F.Kapusta[23], K.Karafasoulis[11], S.Katsanevas[25], E.C.Katsoufis[31], R.Keranen[4], Yu.Khokhlov[41], B.A.Khomenko[16], N.N.Khovanski[16], B.King[22], N.J.Kjaer[30], O.Klapp[51], H.Klein[9], P.Kluit[30], D.Knoblauch[17], P.Kokkinias[11], M.Koratzinos[9], K.Korcyl[18], V.Kostioukhine[41], C.Kourkoumelis[3], O.Kouznetsov[16], M.Krammer[49], C.Kreuter[9], I.Kronkvist[24], J.Krstic[11], Z.Krumstein[16], P.Kubinec[7], W.Kucewicz[18], K.Kurvinen[15], C.Lacasta[9], I.Laktineh[25], J.W.Lamsa[1], L.Lanceri[45], D.W.Lane[1], P.Langefeld[51], J-P.Laugier[38], R.Lauhakangas[15], G.Leder[49], F.Ledroit[14], V.Lefebure[2], C.K.Legan[1], A.Leisos[11], R.Leitner[29], J.Lemonne[2], G.Lenzen[51], V.Lepeltier[19], T.Lesiak[18], M.Lethuillier[38], J.Libby[34], D.Liko[9], A.Lipniacka[43], I.Lippi[35], B.Loerstad[24], J.G.Loken[34], J.M.Lopez[40], D.Loukas[11], P.Lutz[38], L.Lyons[34], J.MacNaughton[49], J.R.Mahon[6], A.Maio[21], T.G.M.Malmgren[43], V.Malychev[16], F.Mandl[49], J.Marco[40], R.Marco[40], B.Marechal[46], M.Margoni[35], J-C.Marin[9], C.Mariotti[9], A.Markou[11], C.Martinez-Rivero[33], F.Martinez-Vidal[48], S.Marti i Garcia[22], F.Matorras[40], C.Matteuzzi[27], G.Matthiae[37], M.Mazzucato[35], M.Mc Cubbin[22], R.Mc Kay[1], R.Mc Nulty[9], G.Mc Pherson[22], J.Medbo[47], C.Meroni[27], W.T.Meyer[1], A.Miagkov[41], M.Michelotto[35], E.Migliore[44], L.Mirabito[25], W.A.Mitaroff[49], U.Mjoernmark[24], T.Moa[43], R.Moeller[28], K.Moenig[9], M.R.Monge[13], X.Moreau[23], P.Morettini[13], K.Muenich[51], M.Mulders[30], L.M.Mundim[6], W.J.Murray[36], B.Muryn[14,18], G.Myatt[34], T.Myklebust[32], F.Naraghi[14], F.L.Navarria[5], S.Navas[48], K.Nawrocki[50], P.Negri[27], S.Nemecek[12], N.Neufeld[9], W.Neumann[51], N.Neumeister[49], R.Nicolaidou[14], B.S.Nielsen[28], M.Nieuwenhuizen[30], V.Nikolaenko[10], M.Nikolenko[10,16], P.Niss[43], A.Nomerotski[35], A.Normand[22], A.Nygren[24], W.Oberschulte-Beckmann[17], V.Obraztsov[41], A.G.Olshevski[16], R.Orava[15], G.Orazi[10], S.Ortuno[48], K.Osterberg[15], A.Ouraou[38], P.Paganini[19], M.Paganoni[9,27], S.Paiano[5], R.Pain[23], H.Palka[18], Th.D.Papadopoulou[31], K.Papageorgiou[11], L.Pape[9], C.Parkes[34], F.Parodi[13], U.Parzefall[22], A.Passeri[39], M.Pegoraro[35], L.Peralta[21], H.Pernegger[49], M.Pernicka[49], A.Perrotta[5], C.Petridou[45], A.Petrolini[13], H.T.Phillips[36], G.Piana[13], F.Pierre[38], M.Pimenta[21], E.Piotto[35], T.Podobnik[34], O.Podobrin[9], M.E.Pol[6], G.Polok[18], P.Poropat[45], V.Pozdniakov[16], P.Privitera[37], N.Pukhaeva[16], A.Pullia[27], D.Radojicic[34], S.Ragazzi[27], H.Rahmani[31], J.Rames[12], P.N.Ratoff[20], A.L.Read[32], M.Reale[51], P.Rebecchi[9], N.G.Redaelli[27], M.Regler[49], D.Reid[9], R.Reinhardt[51], P.B.Renton[34], L.K.Resvanis[3], F.Richard[19], J.Ridky[12], G.Rinaudo[44], O.Rohne[32], A.Romero[44], P.Ronchese[35], E.I.Rosenberg[1], P.Rosinsky[7], P.Roudeau[19], T.Rovelli[5], V.Ruhlmann-Kleider[38], A.Ruiz[40], H.Saarikko[15], Y.Sacquin[38], A.Sadovsky[16], G.Sajot[14], J.Salt[48], D.Sampsonidis[11], M.Sannino[13], H.Schneider[17], U.Schwickerath[17], M.A.E.Schyns[51], G.Sciolla[44], F.Scuri[45], P.Seager[20], Y.Sedykh[16], A.M.Segar[34], A.Seitz[17], R.Sekulin[36], R.C.Shellard[6], A.Sheridan[22], P.Siegrist[9,38], R.Silvestre[38], F.Simonetto[35], A.N.Sisakian[16], T.B.Skaali[32], G.Smadja[25], N.Smirnov[41], O.Smirnova[24], G.R.Smith[36], A.Sokolov[41], O.Solovianov[41], R.Sosnowski[50], D.Souza-Santos[6], T.Spassov[21], E.Spiriti[39], P.Sponholz[51], S.Squarcia[13], D.Stampfer[9], C.Stanescu[39], S.Stanic[42], S.Stapnes[32], I.Stavitski[35], K.Stevenson[34], A.Stocchi[19], J.Strauss[49], R.Strub[10], B.Stugu[4], M.Szczekowski[50], M.Szeptycka[50], T.Tabarelli[27], F.Tegenfeldt[47], F.Terranova[27],

J.Thomas[34], A.Tilquin[26], J.Timmermans[30], L.G.Tkatchev[16], T.Todorov[10], S.Todorova[10], D.Z.Toet[30], A.Tomaradze[2], B.Tome[21], A.Tonazzo[27], L.Tortora[39], G.Transtromer[24], D.Treille[9], G.Tristram[8], A.Trombini[19], C.Troncon[27], A.Tsirou[9], M-L.Turluer[38], I.A.Tyapkin[16], M.Tyndel[36], S.Tzamarias[11], B.Ueberschaer[51], O.Ullaland[9], V.Uvarov[41], G.Valenti[5], E.Vallazza[45], G.W.Van Apeldoorn[30], P.Van Dam[30], J.Van Eldik[30], A.Van Lysebetten[2], I.Van Vulpen[30], N.Vassilopoulos[34], G.Vegni[27], L.Ventura[35], W.Venus[36], F.Verbeure[2], M.Verlato[35], L.S.Vertogradov[16], V.Verzi[37], D.Vilanova[38], P.Vincent[23], L.Vitale[45], E.Vlasov[41], A.S.Vodopyanov[16], V.Vrba[12], H.Wahlen[51], C.Walck[43], C.Weiser[17], A.M.Wetherell[9], D.Wicke[51], J.H.Wickens[2], G.R.Wilkinson[9], W.S.C.Williams[34], M.Winter[10], M.Witek[18], T.Wlodek[19], G.Wolf[9], J.Yi[1], O.Yushchenko[41], F.Zach[25], A.Zaitsev[41], A.Zalewska[18], P.Zalewski[50], D.Zavrtanik[42], E.Zevgolatakos[11], N.I.Zimin[16], G.C.Zucchelli[43], G.Zumerle[35]

[1] Department of Physics and Astronomy, Iowa State University, Ames IA 50011-3160, USA
[2] Physics Department, Univ. Instelling Antwerpen, Universiteitsplein 1, B-2610 Wilrijk, Belgium
and IIHE, ULB-VUB, Pleinlaan 2, B-1050 Brussels, Belgium
and Faculté des Sciences, Univ. de l'Etat Mons, Av. Maistriau 19, B-7000 Mons, Belgium
[3] Physics Laboratory, University of Athens, Solonos Str. 104, GR-10680 Athens, Greece
[4] Department of Physics, University of Bergen, Allégaten 55, N-5007 Bergen, Norway
[5] Dipartimento di Fisica, Università di Bologna and INFN, Via Irnerio 46, I-40126 Bologna, Italy
[6] Centro Brasileiro de Pesquisas Físicas, rua Xavier Sigaud 150, RJ-22290 Rio de Janeiro, Brazil
and Depto. de Física, Pont. Univ. Católica, C.P. 38071 RJ-22453 Rio de Janeiro, Brazil
and Inst. de Física, Univ. Estadual do Rio de Janeiro, rua São Francisco Xavier 524, Rio de Janeiro, Brazil
[7] Comenius University, Faculty of Mathematics and Physics, Mlynska Dolina, SK-84215 Bratislava, Slovakia
[8] Collège de France, Lab. de Physique Corpusculaire, IN2P3-CNRS, F-75231 Paris Cedex 05, France
[9] CERN, CH-1211 Geneva 23, Switzerland
[10] Institut de Recherches Subatomiques, IN2P3 - CNRS/ULP - BP20, F-67037 Strasbourg Cedex, France
[11] Institute of Nuclear Physics, N.C.S.R. Demokritos, P.O. Box 60228, GR-15310 Athens, Greece
[12] FZU, Inst. of Physics of the C.A.S. High Energy Physics Division, Na Slovance 2, 180 40, Praha 8, Czech Republic
[13] Dipartimento di Fisica, Università di Genova and INFN, Via Dodecaneso 33, I-16146 Genova, Italy
[14] Institut des Sciences Nucléaires, IN2P3-CNRS, Université de Grenoble 1, F-38026 Grenoble Cedex, France
[15] Helsinki Institute of Physics, HIP, P.O. Box 9, FIN-00014 Helsinki, Finland
[16] Joint Institute for Nuclear Research, Dubna, Head Post Office, P.O. Box 79, 101 000 Moscow, Russian Federation
[17] Institut für Experimentelle Kernphysik, Universität Karlsruhe, Postfach 6980, D-76128 Karlsruhe, Germany
[18] Institute of Nuclear Physics and University of Mining and Metalurgy, Ul. Kawiory 26a, PL-30055 Krakow, Poland
[19] Université de Paris-Sud, Lab. de l'Accélérateur Linéaire, IN2P3-CNRS, Bât. 200, F-91405 Orsay Cedex, France
[20] School of Physics and Chemistry, University of Lancaster, Lancaster LA1 4YB, UK
[21] LIP, IST, FCUL - Av. Elias Garcia, 14-1^{o}, P-1000 Lisboa Codex, Portugal
[22] Department of Physics, University of Liverpool, P.O. Box 147, Liverpool L69 3BX, UK
[23] LPNHE, IN2P3-CNRS, Universités Paris VI et VII, Tour 33 (RdC), 4 place Jussieu, F-75252 Paris Cedex 05, France
[24] Department of Physics, University of Lund, Sölvegatan 14, S-22363 Lund, Sweden
[25] Université Claude Bernard de Lyon, IPNL, IN2P3-CNRS, F-69622 Villeurbanne Cedex, France
[26] Univ. d'Aix - Marseille II - CPP, IN2P3-CNRS, F-13288 Marseille Cedex 09, France
[27] Dipartimento di Fisica, Università di Milano and INFN, Via Celoria 16, I-20133 Milan, Italy
[28] Niels Bohr Institute, Blegdamsvej 17, DK-2100 Copenhagen 0, Denmark
[29] NC, Nuclear Centre of MFF, Charles University, Areal MFF, V Holesovickach 2, 180 00, Praha 8, Czech Republic
[30] NIKHEF, Postbus 41882, NL-1009 DB Amsterdam, The Netherlands
[31] National Technical University, Physics Department, Zografou Campus, GR-15773 Athens, Greece
[32] Physics Department, University of Oslo, Blindern, N-1000 Oslo 3, Norway
[33] Dpto. Fisica, Univ. Oviedo, Avda. Calvo Sotelo, S/N-33007 Oviedo, Spain, (CICYT-AEN96-1681)
[34] Department of Physics, University of Oxford, Keble Road, Oxford OX1 3RH, UK
[35] Dipartimento di Fisica, Università di Padova and INFN, Via Marzolo 8, I-35131 Padua, Italy
[36] Rutherford Appleton Laboratory, Chilton, Didcot OX11 OQX, UK
[37] Dipartimento di Fisica, Università di Roma II and INFN, Tor Vergata, I-00173 Rome, Italy
[38] CEA, DAPNIA/Service de Physique des Particules, CE-Saclay, F-91191 Gif-sur-Yvette Cedex, France
[39] Istituto Superiore di Sanità, Ist. Naz. di Fisica Nucl. (INFN), Viale Regina Elena 299, I-00161 Rome, Italy
[40] Instituto de Fisica de Cantabria (CSIC-UC), Avda. los Castros, S/N-39006 Santander, Spain, (CICYT-AEN96-1681)
[41] Inst. for High Energy Physics, Serpukov P.O. Box 35, Protvino, (Moscow Region), Russian Federation
[42] J. Stefan Institute, Jamova 39, SI-1000 Ljubljana, Slovenia and Department of Astroparticle Physics, School of Environmental Sciences, Kostanjeviska 16a, Nova Gorica, SI-5000 Slovenia,
and Department of Physics, University of Ljubljana, SI-1000 Ljubljana, Slovenia
[43] Fysikum, Stockholm University, Box 6730, S-113 85 Stockholm, Sweden
[44] Dipartimento di Fisica Sperimentale, Università di Torino and INFN, Via P. Giuria 1, I-10125 Turin, Italy
[45] Dipartimento di Fisica, Università di Trieste and INFN, Via A. Valerio 2, I-34127 Trieste, Italy
and Istituto di Fisica, Università di Udine, I-33100 Udine, Italy
[46] Univ. Federal do Rio de Janeiro, C.P. 68528 Cidade Univ., Ilha do Fundão BR-21945-970 Rio de Janeiro, Brazil
[47] Department of Radiation Sciences, University of Uppsala, P.O. Box 535, S-751 21 Uppsala, Sweden
[48] IFIC, Valencia-CSIC, and D.F.A.M.N., U. de Valencia, Avda. Dr. Moliner 50, E-46100 Burjassot (Valencia), Spain
[49] Institut für Hochenergiephysik, Österr. Akad. d. Wissensch., Nikolsdorfergasse 18, A-1050 Vienna, Austria
[50] Inst. Nuclear Studies and University of Warsaw, Ul. Hoza 69, PL-00681 Warsaw, Poland
[51] Fachbereich Physik, University of Wuppertal, Postfach 100 127, D-42097 Wuppertal, Germany
[52] On leave of absence from IHEP Serpukhov

1 Introduction

In the Standard Model (SM) of the strong (QCD) and electroweak (EW) interactions, the masses of all the fermions, leptons and quarks, are fundamental free parameters. From the perspective of the SM Lagrangian, the mass parameters are effective coupling constants which can be included in the renormalization procedure of the theory. As is well known, several valid renormalization schemes exist, each one postulating a different renormalized mass definition. The perturbative pole mass, M_q, and the running mass, m_q, of the $\overline{MS}$ scheme are among the most attractive mass definitions due to their intrinsic physical properties. The former definition is the renormalized pole of the fermion propagator and is scheme invariant, though naturally prescribed by the on-shell scheme. For free fermions, it corresponds to the usual kinematic mass reconstructed in experiments. The latter definition is purely dynamical, it is associated to the renormalized fermion mass of the $\overline{MS}$ scheme and depends on the energy scale, μ, of the process under study. This last feature, which is not shared by the pole mass, has never been cross-checked by experiment, even though its confirmation is expected by the renormalizable structure of the SM theory and has important implications on the unification of the so called Yukawa couplings.

Heavy fermions show the strongest absolute dependence of the running mass on the energy scale, and hence are the best candidates to test the *running mass* property. At LEP energies this statement suggests the b-quark mass as the experimental target of such an analysis and QCD as the proper theoretical scenario. Mass determinations are, in general, more complicated and less precise for quarks than for leptons because the use of dynamical relations to unfold the strong bounding forces between them is mandatory, since stable quarks exist only in bound states.

Up to now, the b quark mass has been extracted from the known spectra of the hadronic bound states of the Υ resonances, for example by using QCD sum rules or lattice calculations [1]. The b pole mass measured with these methods is $M_b \approx 4.7$ GeV/c^2, and the b running mass is $m_b(\mu) \approx 4.2$ GeV/c^2 at $\mu = m_b$. The change of this value at the LEP energy scale, $\sqrt{s} \sim M_Z$, is predicted by QCD to be $(m_b(M_Z) - m_b(m_b)) \sim -1.2$ GeV/c^2.

At LEP energies, b quark mass effects usually appear in terms proportional to m_b^2/M_Z^2 ($\lesssim$0.003) and can be safely neglected for many observables, for instance for the total hadronic cross-section. But for other specific quantities, like the differential multi-jet cross-section for b events, the mass corrections are sizeable because they are of the form $m_b^2/M_Z^2/y_c$, where y_c is the jet-resolution parameter ($\sim$0.01).

Calculations including mass terms at Leading Order (LO) for three- and four-jet event rates [2,3] have been used in tests of the universality of the strong coupling constant for b events, α_s^b [4,5]. A suppression of $\sim$5% [2–4] is predicted for the three-jet cross-section for b-quark events with respect to that for light-quark ($\ell \equiv u, d, s$) events. The exact amount of this suppression depends of course on m_b, y_c, and the jet reconstruction algorithm chosen. However these calculations could not be used to evaluate m_b itself, because they contain only LO terms with no need for any particular renormalization processing. As no renormalization information was required, no physical argument could be developed to identify the mass parameter appearing in these expressions consistently as being either the pole mass or the running mass.

Recently, Next to Leading Order (NLO) calculations of the multi-jet production rate [6–9] have become available. They solve this mass ambiguity because they include radiative loop corrections. They thus permit a proper determination of m_b. The proposed

observable is [4,7,10]:

$$R_3^{b\ell}(y_c) = \frac{\Gamma_{3j}^{Z\to b\bar{b}g}(y_c)/\Gamma_{tot}^{Z\to b\bar{b}}}{\Gamma_{3j}^{Z\to \ell\bar{\ell}g}(y_c)/\Gamma_{tot}^{Z\to \ell\bar{\ell}}} = 1 + r_b(\mu)\cdot\left(b_I(y_c, r_b(\mu)) + \frac{\alpha_s(\mu)}{\pi}\cdot b_{II}(y_c, r_b(\mu))\right) \quad (1)$$

where $\Gamma_{3j}^{Z\to q\bar{q}g}$ and $\Gamma_{tot}^{Z\to q\bar{q}}$ are the differential three-jet and total cross-sections, respectively, for the b ($q = b$) and light ($q = \ell \equiv u, d, s$) quarks. The functions b_I and b_{II} can be found in reference [7] and the parameter $r_b(\mu)$ is $m_b^2(\mu)/M_Z^2$.

This letter presents the DELPHI measurement of m_b at the M_Z scale using $R_3^{b\ell}(y_c)$ as the directly observed quantity and Eq. (1) as the expression for extracting m_b. The comparison of this result with the value of m_b obtained from the Υ resonances represents the first experimental attempt to establish the *running property* of the b quark mass.

2 Detector description

The DELPHI detector, surrounding one of the interaction regions at the Large Electron Positron facility LEP at CERN, has been used to record the samples of events considered in this analysis. It provides both tracking and calorimetric information over almost the full solid angle. A detailed description of the detector and its performance, including the exact geometry as well as the trigger conditions and the event processing chain, appear in references [11,12].

The barrel region of the detector consists of a system of cylindrical tracking detectors and an electromagnetic calorimeter, within a superconducting solenoidal coil providing a uniform magnetic field of 1.23 T parallel to the beam direction (z). The central tracking detectors, Vertex Detector (VD), Inner Detector (ID), Time Projection Chamber (TPC) and Outer Detector (OD), provide measurements of charged particles tracks both in the $r\phi$ plane, transverse to the beam, and in the z direction. The VD consists of three concentric layers of silicon microstrip detectors. In 1994 this detector was upgraded and two of the layers were replaced by double-sided silicon microstrip detectors. The ID is a cylindrical jet chamber surrounded by five layers of multi-wire proportional chambers. The TPC is the main tracking device, which also provides information on energy loss, dE/dx. The tracking in the barrel region is completed by the OD which is composed of five layers of drift cells and in the endcaps by further tracking Forward Chambers, FCA and FCB. The DELPHI tracking system provides an average momentum resolution of $\sigma(p)/p = 3.6\%$ for muons of 45 GeV/c.

The electro-magnetic calorimetry is accomplished by the High Density Projection Chamber (HPC) and the Forward Electromagnetic Calorimeter (FEMC) that correspond to the barrel and forward region, respectively. Their information allows electron and photon identification. Muons are identified by the muon detector system, consisting of several layers of drift chambers located within and beyond the outer layers of the hadron calorimeter (HAC), which also serves as the return yoke of the magnet.

3 Event selection

All data collected by DELPHI during 1992, 1993 and 1994 were considered in the present analysis and corresponded to centre-of-mass energies of $\sqrt{s} \approx M_Z$. In a first step of the selection procedure, quality cuts were imposed on all charged particles and all neutral clusters in the calorimeters in order to ensure a reliable determination of their

kinematic variables, momenta and energies. The charged particles entering in the analysis were all assumed to be pions. They were required to be well contained within the detector acceptance and to originate close to the interaction point (IP). Neutral clusters reconstructed in the HPC, FEMC and HAC were selected by imposing conditions on the minimum reconstructed energy, with an additional requirement on the distribution of the layers hit for HPC clusters. Identified electron positron pairs arising from photon conversions were considered as single neutral clusters if the sum of their momenta exceeded 600 MeV/c.

A sample of hadronic events was then selected by demanding a minimum charged particle multiplicity and enough visible energy carried by charged particles well contained within the detector volume, and by vetoing events having poorly measured particles. The retained data sample contained $\sim 2.5 \cdot 10^6$ hadronic Z decays with a small contamination from $\tau^+\tau^-$ pairs ($\sim 1‰$) and a negligible background from beam-gas scattering and $\gamma\gamma$ interactions. The specific cuts used are presented in Table 1.

Charged Particle Selection	$p \geq 0.1$ GeV/c, $\quad \Delta(p)/p \leq 1$ $25° \leq \theta \leq 155°$ L$\geq$ 50 cm $\delta \leq 5$ cm in $r\phi$ plane $\delta \leq 10$ cm in z direction	
Neutral Cluster Selection	$E \geq 0.8$ GeV, $\ 40° \leq \theta \leq 140°$ $E \geq 0.5$ GeV, $\ 8°(144°) \leq \theta \leq 36°(172°)$ $E \geq 1.5$ GeV, $\ 10° \leq \theta \leq 170°$	HPC FEMC HAC
Event Selection	$N_{ch} \geq 5$ $E_{ch} \geq 15$ GeV $\lvert \sum_i q_i \rvert \leq 6$, $i = 1, .., N_{ch}$ No particle with $E \geq 40$ GeV $40° \leq \theta_{thrust} \leq 140°$	

Table 1: Particle and hadronic event selection; p is the particle momentum, θ the particle (and θ_{thrust} the *thrust*) polar angle with respect to the beam axis, L the measured track length, δ the closest distance to the IP, q_i the particle charge, E the cluster energy, N_{ch} the number of charged particles, and E_{ch} the total charged particle energy in the event.

The charged and neutral particles of each selected event were then grouped into jets by means of the DURHAM jet finding algorithm [13], whose definition and main properties appear in Table 2. For each pair of particles ij, the DURHAM jet resolution variable y_{ij} was calculated from their four-momentum vectors. The pair with the smallest y_{ij} that did not exceed the resolution parameter, y_c, was combined to form a new pseudo-particle with four-momentum $p_k = p_i + p_j$. The procedure was iterated until no further pairs of particles or pseudo-particles satisfied the condition $y_{ij} \leq y_c$. The particles or pseudo-particles remaining were henceforth called jets, and their number determined the class of the event (two-jet, three-jet, etc.).

The accepted events were well identified hadronic events, but their kinematics could still be affected by particle losses and wrong energy-momentum assignment to the jets. In order to ensure good energy balance in these events, further quality cuts were applied using the reconstructed jet information. For each event, the largest y_c value that would

Algorithm	Reference	Resolution	Recombination
DURHAM	[13]	$y_{ij} = \frac{2\cdot\min(E_i^2,E_j^2)\cdot(1-\cos\theta_{ij})}{E_{vis}^2}$	$p_k = p_i + p_j$

Table 2: Definition of the jet resolution variable y_{ij} of the DURHAM recombination scheme; E_{vis} is the total visible energy of the event, $p_i \equiv (E_i, \vec{p}_i)$ denotes a 4-vector and θ_{ij} is the angle between $\vec{p}_i$ and $\vec{p}_j$.

classify it as a three-jet event was determined. The jet energies were then re-calculated using the angular separations between the jets using the triangle relation [14] and the conditions listed in Table 3 were imposed. A total of $1.9\cdot10^6$ hadronic events passed these criteria and the $\tau^+\tau^-$ pair contamination was further reduced to be less than $0.01‰$.

Kinematic Selection	$N_{ch} \geq 1$ per jet $E_j \geq 3$ GeV, $\quad j = 1,2,3$ $25° \leq \theta_j \leq 155°, \quad j = 1,2,3$ Planarity cut: $\sum_{ij} \phi_{ij} \geq 359°, \quad i<j, \quad i,j = 1,2,3$

Table 3: Event selection based on the kinematic properties of the events when clustered in three-jets by the DURHAM algorithm; E_j is the jet energy, θ_j is the jet polar angle and ϕ_{ij} the angular separation between the pair of jets ij.

The lifetime-signed impact parameters of charged particles were used to construct an algorithm for tagging b-quark and ℓ-quark events [15,16]. In this method the probability, P, for the hypothesis that an event contained no decay products from long lived hadrons was evaluated using all of the selected charged particle tracks that had positive impact parameter. By construction, ℓ-quark events gave an almost flat P distribution while b-quark events gave small values of P. Hence P could be used to discriminate the flavour of the event. The $\mathrm{Log}_{10}(\mathrm{P})$ distribution is shown in Fig. 1 for real data and simulated events [12]. A good agreement between real and simulated data can be observed.

Each value of P corresponds to a well determined combination of purity and efficiency [16] for either b or ℓ events. The cut on P to select b candidates was fixed to $\mathrm{P} \leq 5\cdot10^{-3}$. The purity and efficiency achieved were around 85% and 55% respectively (different for each year). To select light quarks, P was required to exceed 0.2, leading to about 80% purity and $\sim 80\%$ efficiency. The numbers of b-quark and ℓ-quark events finally selected are itemized in Table 4, together with the flavour composition of each sample, *i.e.* the purity and the contamination, according to results derived from the DELPHI detector simulation [12].

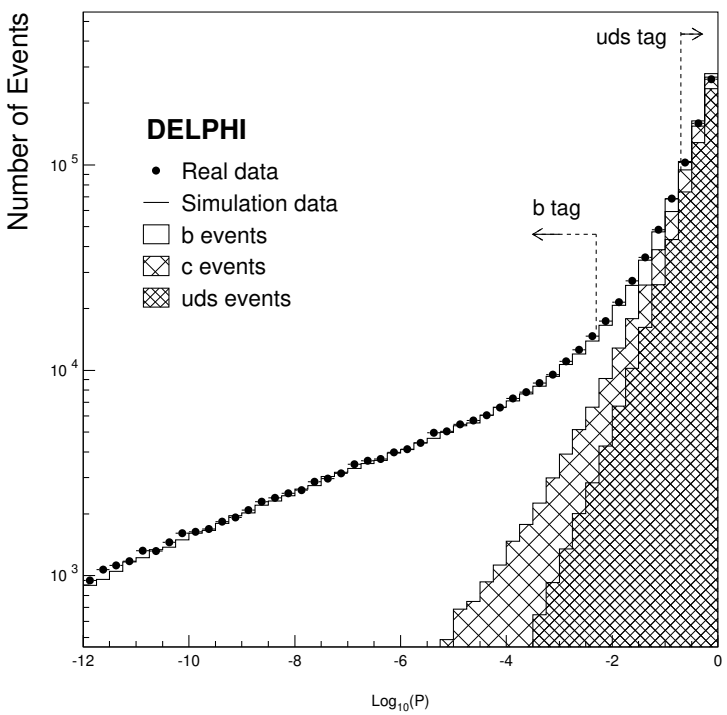

Figure 1: Event distribution of the logarithm of the probability to contain no secondary vertices (P). The 1994 real data (points) and simulated data (histograms) are compared. The specific contribution of each quark flavour is displayed as derived from the simulation. The cuts used to tag the b-quark and light-quark ($\ell \equiv u, d, s$) samples are also indicated.

4 Experimental strategy

The normalized measured three-jet cross-sections, $R_{3q}^{mes}(y_c) = \Gamma_{3j-mes}^{Z\to q\bar{q}g}(y_c)/\Gamma_{tot-mes}^{Z\to q\bar{q}}$ with $q \equiv b$ and ℓ, were computed as well as their ratio,

$$R_3^{b\ell-mes}(y_c) \;=\; \frac{R_{3b}^{mes}(y_c)}{R_{3\ell}^{mes}(y_c)}.$$

A sample of $\sim 4\cdot 10^6$ simulated events was then used to correct this measured value for detector acceptance effects, kinematic biases introduced in the tagging procedure, and the hadronization process, and thus to transform this raw ratio into the quark-parton result equivalent to the theoretical expectation of Eq. (1). The sample was generated using the JETSET 7.3 Parton Shower (PS) Monte Carlo [17] and passed through the full simulation and reconstruction of DELPHI [12]. The above analysis was applied to the simulated events, and the normalized three-jet cross-sections were defined for each set of tagged events, in the same way as for the real data. In this case, however, the contribution of each quark flavour to the measured normalized three-jet cross-section could be quantified according to

$$\begin{aligned} R_{3b}^{mes-sim}(y_c) &= R_{3b}^{b-sim}(y_c)\cdot c_b^b + R_{3b}^{\ell-sim}(y_c)\cdot c_b^\ell + R_{3b}^{c-sim}(y_c)\cdot c_b^c \\ R_{3\ell}^{mes-sim}(y_c) &= R_{3\ell}^{b-sim}(y_c)\cdot c_\ell^b + R_{3\ell}^{\ell-sim}(y_c)\cdot c_\ell^\ell + R_{3\ell}^{c-sim}(y_c)\cdot c_\ell^c \end{aligned} \qquad (2)$$

# ev. in data	q-type	$\ell \to q$-type (%)	$c \to q$-type (%)	$b \to q$-type (%)
1,074,860	ℓ	80.2 $\pm$ 1.8	15.1 $\pm$ 0.6	4.7$\pm$1.1
294,509	b	5.1 $\pm$ 0.3	10.1 $\pm$ 2.1	84.8 $\pm$2.4

Table 4: Final sizes and flavour compositions of the samples tagged as light ($\ell \equiv u, d, s$) and b-quark events. The compositions were extracted from simulation and corresponded to the average values obtained after gathering all years' data. The quoted errors indicate the variation of the mean values from year to year, due mainly to the VD upgrade in 1994.

where $R_{3q}^{mes-sim}(y_c)$ was the simulated normalized three-jet cross-section of each data sample equivalent to the measured quantity, the $R_{3q}^{i-sim}(y_c)$ ($i = b, c, \ell$) corresponded to the normalized three-jet cross-section of each quark flavour, and the weights c_q^i corresponded to the compositions listed in Table 4. The flavour assignment, i, of the events entering in the terms $R_{3q}^{i-sim}(y_c)$ was defined to be the flavour of the pair of quarks coupled to the Z which initiated the parton shower. This avoided flavour misidentification ambiguities due to the gluon splittings into quarks occurring during the parton shower evolution. The same convention was considered in the theoretical calculation of [7], thus allowing a consistent comparison.

Detector and acceptance effects plus kinematic biases, $d(y_c)$, and hadronization effects, $h(y_c)$, were then computed for each term of Eq. (2) as multiplicative factors connecting the normalized three-jet cross-sections R_{3q}^{i-sim} with their related parton level quantities, R_{3q}^{i-par}, as

$$R_{3q}^{i-sim}(y_c) \;=\; d_{3q}^{i}(y_c) \cdot h_{3q}^{i}(y_c) \cdot R_{3q}^{i-par}(y_c).$$

Different $d(y_c)$ factors were calculated for each year in order to take changes in the detector configuration into account. The $h(y_c)$ factors were taken from the tuned DELPHI parameters appearing in [18].

The effect of the c-quark mass was neglected as it is only about 10% ($\sim m_c^2/m_b^2$) of that of the b-quark mass. Thus the normalized three jet cross-section of c quarks at parton level was assumed to be equal to that of light quarks, *i.e.*, $R_{3q}^{c-par} = R_{3q}^{\ell-par}$. The simulated *measured* quantities are then related to the *parton* ones as follows:

$$\begin{aligned} R_{3b}^{mes-sim}(y_c) &= A_b(y_c) \cdot R_{3b}^{par}(y_c) + B_b(y_c) \cdot R_{3\ell}^{par}(y_c) \\ R_{3\ell}^{mes-sim}(y_c) &= A_\ell(y_c) \cdot R_{3b}^{par}(y_c) + B_\ell(y_c) \cdot R_{3\ell}^{par}(y_c) \end{aligned} \tag{3}$$

where the parameters A_b, B_b, A_ℓ, B_ℓ are a more compact re-definition of the original set of parameters: $d_{3q}^i, h_{3q}^i, c_q^i$. The values of these parameters were then used to express $R_3^{b\ell-par}$ as a function of $R_3^{b\ell-mes}$ according to

$$R_3^{b\ell}(y_c) \;=\; R_3^{b\ell-par}(y_c) \;=\; \frac{R_{3b}^{par}(y_c)}{R_{3\ell}^{par}(y_c)} \;=\; \frac{B_b(y_c) - B_\ell(y_c) \cdot R_3^{b\ell-mes}(y_c)}{A_\ell(y_c) \cdot R_3^{b\ell-mes}(y_c) - A_b(y_c)} \tag{4}$$

which could then be compared with the theoretical prediction of Eq. (1).

The overall correction to the observed value of $R_3^{b\ell-mes}(y_c)$ was about 10% (averaged over all years) from which $\sim$1% was due to the hadronization process. All years' data sets after correction agreed with each other within one standard deviation of the statistical error. Therefore they were combined without further requirements. Fig. 2 shows the

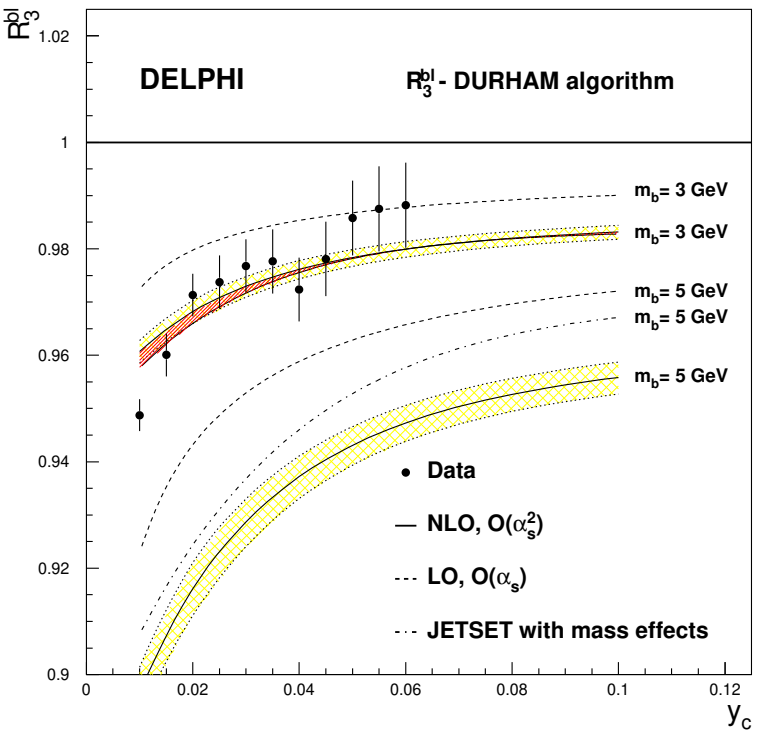

Figure 2: Corrected data values of $R_3^{b\ell-par}(y_c)$ (black points) compared with the theoretical predictions. The dashed lines indicate the LO ($\mathcal{O}(\alpha_s)$) predictions from references [2,3]. The solid lines are the NLO ($\mathcal{O}(\alpha_s^2)$) calculation of reference [7]. The dotted lines contain the area corresponding to a scale interval of $0.5 \leq \mu/M_Z \leq 2$. The range of predictions for the NLO [7,8] for m_b=3 GeV/c^2 with scale $\mu = M_Z$ is shown hatched. The dashed-dotted curve shows the JETSET behaviour for m_b=5 GeV/c^2 when mass effects are included.

corrected data values of $R_3^{b\ell-par}(y_c)$ obtained using Eq. (4), together with the theoretical expectations at LO ($\mathcal{O}(\alpha_s)$) from references [2,3] and at NLO ($\mathcal{O}(\alpha_s^2)$) from references [7,8] for m_b mass values of 3 GeV/c^2 and 5 GeV/c^2 in both cases.

The two recent NLO calculations [7] and [8] agree well, even though they use slightly different definitions of the observable $R_3^{b\ell}(y_c)$. However, only events which have two reconstructed $b\bar{b}$-jets originating from a split gluon contribute to such differences. The effect on R_3^{bl} was studied using JETSET 7.3. First it was checked that the perturbative calculations from [7,19] were reasonably well described by this generator. Secondly, the effect on R_3^{bl} of reconstructing two separate $b\bar{b}$-jets produced by the same split gluon was evaluated. As a function of y_c, the gluon splitting probability into two b-quarks changed R_3^{bl} by approximately +0.002 to +0.006, which was further reduced by the probability of both quarks being reconstructed. This probability varied from 30% to 15%, depending again on y_c. The net effect was therefore below 1‰, which explains the nice agreement which is observed in Fig. 2 between the two theoretical approaches. The data shown in Fig. 2 were also corrected to account for the contribution of anomalous triangle diagrams to the three-jet final state [20]. This contribution was about $\sim$+2‰ for R_3^{bl}.

5 Systematic errors

The study of systematic uncertainties mainly used the JETSET 7.3 event generator. This program contains mass effects based on LO perturbative calculations [21] which govern the emission of hard gluons; in the rest of the phase space, the soft gluon radiation region, only kinematics are considered. The default value of m_b employed by this program is 5 GeV/c^2, which represents a sufficiently good approximation to describe data for most of the present LEP analyses. The R_3^{bl} ratio predicted by this model is also shown in Fig. 2.

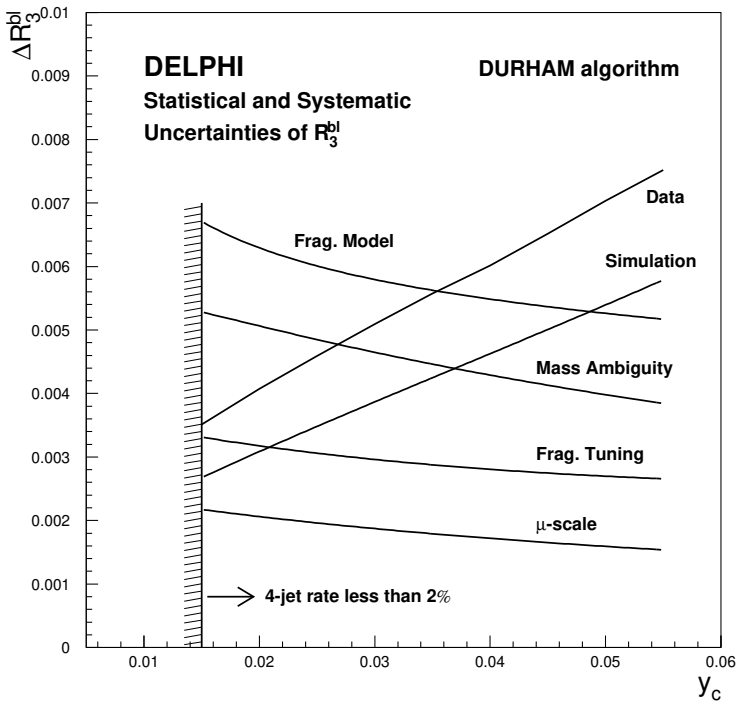

Figure 3: Statistical and systematic uncertainties affecting R_3^{bl} as a function of y_c. The theoretical mass ambiguity and μ-scale uncertainties are not specific errors of R_3^{bl} as they enter only when $m_b(M_Z)$ is calculated from it, but are shown for comparison purposes.

The evaluation of the hadronization correction factors to R_3^{bl} by means of the $O(\alpha_s^2)$ ME (Matrix Element) expressions as they exist in JETSET was discarded because a) the expressions use the massless approximation, b) in this scenario, the multi-jet production rate after fragmentation is strongly influenced by the jet transverse momentum parameter σ_q, which is the same for all flavours. On the contrary, the Parton Shower (PS) option includes some more refined approximation to the massive approach and, in addition, σ_q is less relevant to the multi-jet production rate after fragmentation. The reliable use of the PS model in this analysis is however restricted to the y_c region where the two- and three-jet event rates dominate. Therefore $y_c > 0.015$ was required, which guaranteed that the four-jet production rate was lower than 2%.[2]

The possible dependence of the correction factors on the assumed value of the b mass was also studied. With the present configuration of JETSET this was technically diffi-

[2] The four-jet production rate varied from 5% for $y_c = 0.01$ to 1.5% for $y_c = 0.02$.

cult, as the program uses the same value of m_b to describe both hard and soft processes. A too small value of m_b could lead to unreliable results, e.g. to an unphysical description of B hadron decays. The dependence was therefore tested indirectly by switching the mass effects on and off. This altered the proportion of three-jet b events at parton level without changing the fragmentation process. The number of three-jet b events after fragmentation was seen to scale with the corresponding number at parton level. Therefore, no variation of the correction factors was observed within the statistical precision of the comparison ($\sim 1‰$).

The description of the parton shower evolution is also not unique, and various schemes describe the data reasonably well. The distributions for R_3^{bl} obtained when correcting either by JETSET 7.3 PS [17] or by HERWIG 5.8 [22] were compared using samples of generated events that contained more than 10^7 events. Both programs were seeded with the best set of parameters tuned by DELPHI [18], which also agree well with those found by ALEPH [23]. The corrected R_3^{bl} distributions obtained using JETSET or HERWIG differed by about 1%. The correction adopted was the average of those from the two models and the *fragmentation model* uncertainty was taken to be half of their difference. The data shown in Fig. 2 were corrected using this method. The dependence of the fragmentation model error on y_c can be seen in Fig. 3.

Another source of systematic errors is induced by the lack of exact knowledge of the *fragmentation parameters* of JETSET. Again, huge samples of simulated events were generated (10^7 events per b and ℓ flavour and per parameter) in order to study the particular effect of each JETSET parameter relevant to this analysis: Q_0, σ_q, ϵ_b, a and b. Each of these parameters was assumed to take the optimum value found in the DELPHI tuning [18] and varied by $\pm 2\sigma$ from its central value. None of the individual uncertainties associated with the cited parameters affected the R_3^{bl} determination by more than $2‰$ for y_c values in the region $y_c > 0.01$. The global error given in Fig. 3 was calculated by adding each individual contribution in quadrature neglecting the correlation. In this way, the error associated with the uncertainty of the tuned fragmentation parameters was conservatively estimated to be approximately ± 0.003.

The impact on R_3^{bl} of taking R_{3q}^{c-par} equal to $R_{3q}^{\ell-par}$ was found to be negligible.

The defects of the DELPHI *detector simulation* when trying to reproduce the real data were also considered in the analysis and regarded as an additional source of error. The main contribution to this uncertainty came from the limited statistics of the fully simulated events and the uncertainty in the compositions of the b-tagged and ℓ-tagged samples. The size of this error was derived by solving Eq. (4) when the different flavour contributions (c_{3q}^q) were changed individually by 1% but keeping $\Sigma_q c_{3q}^q = 1$, and by calculating the statistical precision of the simulated sample. The overall error is shown in Fig. 3 and is dominated by the limited statistics available.

6 Results and discussion

The corrected values of $R_3^{b\ell}$ are shown in Fig. 2 as a function of y_c. All data points at different y_c values are highly correlated. The measurement of m_b was therefore based on a single point. The optimization of the statistical error advised the use of small y_c values, but y_c had to lie in a region where the non-perturbative effects and the contributions due to final states with more than three jets were small ($y_c > 0.015$). From the curves shown in Fig. 3, the value $y_c = 0.02$ was chosen, though any value in the range $0.015 \leq y_c \leq 0.03$ was equally valid as their total errors are approximately the same and furthermore their $R_3^{b\ell}$ values are fully compatible, as seen in Fig. 2. The corresponding $R_3^{b\ell}$ value is presented

in Table 5 together with the break-down of the individual errors. The result is

$$R_3^{b\ell}(0.02) = 0.971 \pm 0.005 \text{ (stat.)} \pm 0.007 \text{ (frag.)}, \quad (5)$$

where the statistical errors from the data and the simulation have been added and the fragmentation error accounts for the uncertainties arising from both the fragmentation model and the tuning parameters.

$y_c = 0.02$		
	R_3^{bl}	$m_b(M_Z)$ GeV/c^2
Value	0.971	2.67
Statistical error	± 0.004	± 0.20
Simulation error	± 0.003	± 0.15
Fragmentation Model error	± 0.006	± 0.30
Fragmentation Tuning error	± 0.003	± 0.15
Mass Ambiguity error	–	± 0.25
μ-scale error ($0.5 \leq \mu/M_Z \leq 2$)	–	± 0.10

Table 5: Values of $R_3^{b\ell}$ and $m_b(M_Z)$ and break-down of their associated errors (statistical and systematic) for $y_c = 0.02$.

Additional theoretical uncertainties enter when the measurement of R_3^{bl} is transformed into a determination of $m_b(M_Z)$ by means of Eq. (1). In Fig. 3 they are shown associated to R_3^{bl} for comparison purposes. Firstly, as also happens for α_s measurements, there is an unphysical *μ-scale dependence* which needs to be quantified. In addition, there is a *mass ambiguity* arising from the fact that there are two ways of expressing Eq. (1) in terms of the running b mass at the M_Z scale [7,24]. This latter uncertainty is labelled as the mass ambiguity in Fig. 3 and it reflects the ambiguity of writing Eq. (1) either directly in terms of the running mass at the M_Z scale or using the pole mass as an intermediate stage, transforming it to the running mass at the pole mass scale, M_b, and then making the evolution to the M_Z scale using the renormalization group equations. Both ways are equally valid, but the contributions due to the higher order terms enter differently in the two procedures because truncated and resummed expressions are used differently. The average of the two results was taken and their difference provides an estimate of the unknown higher order contributions.

The result thus obtained for m_b at $\mu = M_Z$ was

$$m_b(M_Z) = 2.67 \pm 0.25 \text{ (stat.)} \pm 0.34 \text{ (frag.)} \pm 0.27 \text{ (theo.) GeV/c}^2,$$

where the statistical and fragmentation errors correspond to the errors expressed for $R_3^{b\ell}$ in Eq. (5) and the theoretical error includes the *mass ambiguity* uncertainty (0.25 GeV/c^2) and the variation of the *scale* in the range $0.5 \leq \mu/M_Z \leq 2$ (0.10 GeV/c^2). Evolving this result down to the b mass scale using $\alpha_s = 0.118 \pm 0.003$ would give $m_b(m_b) = 3.91 \pm 0.67$ GeV/c^2.

Another approach to establishing the theoretical error is reported in [7]. There, Eq. (5) is considered only in terms of the running mass, using the argument that this is a true short distance parameter, as opposed to the pole mass which contains all the complicated

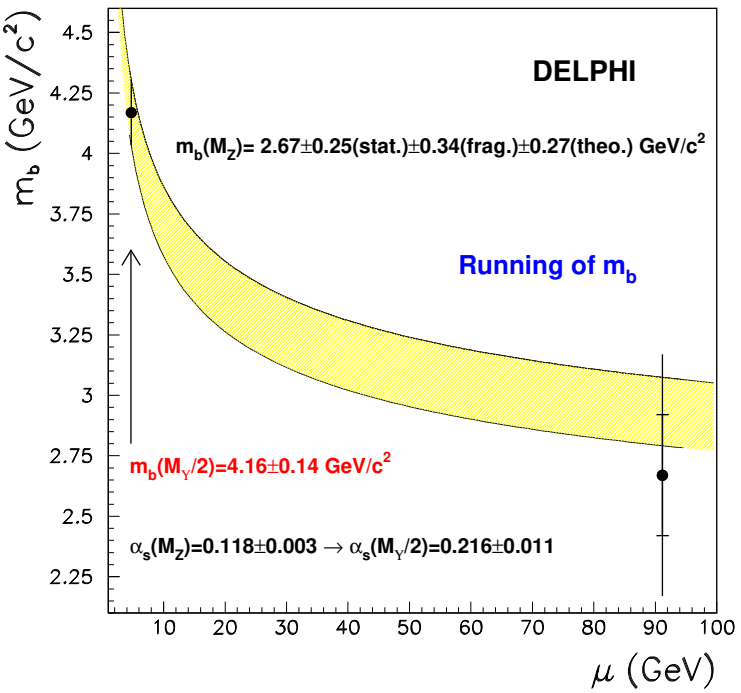

Figure 4: The running of $m_b(\mu)$. The $m_b(M_Z)$ value is displayed together with the statistical and total errors. The hatched area corresponds to the band associated to $m_b(\mu)$ when running the non-weighted average value of $m_b(\mu)$ at $M_\Upsilon/2$ up to the M_Z scale using $\alpha_s(M_Z) = 0.118 \pm 0.003$ [25] and the QCD renormalization group equations.

non-perturbative physics at scales $\mu \sim M_b$. The only error left is then the variation of the scale in the interval from $\mu = 5$ GeV to $\mu = M_Z$. The theoretical error induced by this approach is $\sim$0.20 GeV/c^2 ($+0.10$ GeV/c^2 and -0.30 GeV/c^2) because the dependence on μ is stronger in this case. The result obtained using this method is $m_b(M_Z) = 2.81$ GeV/c^2 at $\mu = (M_Z{+}5)/2$, which is fully compatible with the above result and constitutes a check of consistency.

Assuming all errors to be independent, they were added in quadrature and the values of the running b mass at the M_Υ and M_Z scales were compared. The measured difference between them is

$$m_b(M_Z) - m_b(M_\Upsilon/2) = -1.49 \pm 0.52 \text{ GeV/c}^2,$$

where the value of $m_b(M_\Upsilon/2) = 4.16 \pm 0.14$ GeV/c^2 has been calculated as the non-weighted average of all the results appearing in reference [1] at $\mu = M_\Upsilon/2$.

The observed change of the running b mass value from $M_\Upsilon/2$ to M_Z is an effect of almost three standard deviations and represents the first experimental evidence of the running property of any fermion mass. The result is in good agreement with the predicted QCD evolution, as Fig. 4 shows, and confirms that QCD radiative corrections including mass effects describe the data correctly from the $M_\Upsilon/2$ scale to the M_Z scale.

The result can also be interpreted as a test of the flavour independence of the strong coupling constant by using the relation [13,24]

$$\frac{\alpha_s^b}{\alpha_s^\ell} = R_3^{b\ell} - H(m_b(M_Z)) + 1.94\frac{\alpha_s(M_Z)}{\pi}\left(R_3^{b\ell} - H(m_b(M_Z)) - 1\right), \qquad (6)$$

where α_s^b and α_s^ℓ represent the strong coupling constants for b and ℓ quarks respectively, and $H(m_b(M_Z))$ is the mass correction term of Eq. 1. At $y_c = 0.02$ the value of $H(m_b(M_Z))$ is -0.036 ± 0.005, where the error takes into account the theoretical uncertainties due to the μ scale and to the mass ambiguity as discussed above. Combining this value with that obtained for $R_3^{b\ell}$ from Eq. 5 yields

$$\frac{\alpha_s^b}{\alpha_s^\ell} = 1.007 \pm 0.005 \text{ (stat.)} \pm 0.007 \text{ (frag.)} \pm 0.005 \text{ (theo.)}, \tag{7}$$

which verifies the flavour independence of the strong coupling constant for b and light quarks.

Acknowledgements

We are greatly indebted to our technical collaborators and to the funding agencies for their support in building and operating the DELPHI detector, and to the members of the CERN-SL Division for the excellent performance of the LEP collider. We also thank to G. Rodrigo and A. Santamaría for an enjoyable collaboration with plenty of useful and lively discussions, as well as to P. Nason for his interesting comments on the paper. Furthermore we acknowledge M. Seymour and T. Sjöstrand for their help in understanding the mass effects considered in the HERWIG and JETSET generators.

References

[1] C.A. Dominguez, G.R. Gluckman, N. Paver, Phys. Lett. **B293** (1992) 197 and hep-ph/9410362;
S. Narison, Phys. Lett. **B341** (1994) 73;
M. Neubert, Phys. Rep. **245** (1994) 259 and hep-ph/9404296;
S. Titard, F. J. Yndurain, Phys. Rev **D49** (1994) 6007;
M. Jamin, A. Pich, IFIC-97-06, FTUV-97-06, HD-THEP-96-55, hep-ph/9702276;
M. Crisafulli, V. Giménez, G. Martinelli, C.T. Sachrajda, Nucl. Phys. **B457** (1995) 594;
V. Giménez, G. Martinelli, C.T. Sachrajda, Nucl. Phys. Proc. Suppl. **53** (1997) 365 and Phys. Lett. **B393** (1997) 124 ;
C.T.H. Davies et al., Phys. Rev. Lett. **73** (1994) 2654 and Phys. Lett. **B345** (1995) 42.

[2] A. Ballestrero, E. Maina, S. Moretti, Phys. Lett. **B294** (1992) 425 and Nucl. Phys. **B415** (1994) 265.

[3] M. Bilenky, G. Rodrigo, A. Santamaría, Nucl. Phys. **B439** (1995) 505.

[4] DELPHI Coll., P. Abreu et al., Phys. Lett. **B307** (1993) 221;
J. Chrin, Proc. 28th Rencontre de Moriond, 1993, p. 313, ed. J.T.T. Van;
J. Valls, PhD Thesis, Universitat de València, 1994, unpublished.

[5] L3 Coll., B. Adeva et al., Phys. Lett. **B263** (1991) 551;
OPAL Coll., R. Akers et al., Z. Phys. **C65** (1995) 31;
ALEPH Coll., D. Buskulic et al., Phys. Lett. **B355** (1995) 381;
SLD Coll., K. Abe et al., SLAC-PUB-7573, Jan. 1997.

[6] G. Rodrigo, QCD-96 Montpellier, hep-ph/9609213 and Nucl. Phys. Proc. Suppl. **54A** (1997) 60.

[7] G. Rodrigo, M. Bilenky, A. Santamaría, Phys. Rev. Lett. **79** (1997) 193.

[8] W. Bernreuther, A. Brandenburg, P. Uwer, Phys. Rev. Lett. **79** (1997) 189.
[9] P. Nason and C. Oleari, Phys. Lett. **B407** (1997) 57.
[10] J. Fuster, S. Cabrera, S. Martí i García, QCD-96 Montpellier, hep-ex/9609004 and Nucl. Phys. Proc. Suppl. **54A** (1997) 39.
[11] DELPHI Coll., P. Aarnio et al., Nucl. Instr. Meth. **A303** (1991) 233.
[12] DELPHI Coll., P. Abreu et al., Nucl. Instr. Meth. **A378** (1996) 57.
[13] S. Catani et al., Phys. Lett. **B269** (1991) 432;
N. Brown, W.J. Stirling, Z. Phys. **C53** (1992) 629.
[14] DELPHI Coll., P. Abreu et al., Z. Phys. **C70** (1996) 179.
[15] ALEPH Coll., D. Buskulic et al., Phys. Lett. **B313** (1993) 535.
[16] G.V. Borisov, Lifetime Tag of Events with B-hadrons with the DELPHI detector, preprint IHEP (Protvino) 94-98 (1994);
DELPHI Coll., P. Abreu et al., Z. Phys. **C65** (1995) 555;
G.V. Borisov, C. Mariotti, Nucl. Instr. Meth. **A372** (1996) 181.
[17] T. Sjöstrand, Comp. Phys. Comm. **39** (1986) 346.
[18] DELPHI Coll., P. Abreu et al., Z. Phys. **C73** (1996) 11.
[19] M. H. Seymour, Nucl. Phys. **B436** (1995) 163 and Z. Phys. **C63** (1994) 99;
M.L. Mangano, P. Nason, Phys. Lett **B285** (1992) 160.
[20] K. Hagiwara, T. Kuruma, Y. Yamada, Nucl. Phys. **B358** (1991) 80.
[21] B.L. Ioffe, Phys. Lett. **B78** (1978) 277.
[22] G. Marchesini et al., Comp. Phys. Comm. **67** (1992) 465.
[23] ALEPH Coll., R. Barate et al., CERN-PPE-96-186.
[24] G. Rodrigo, PhD Thesis, Universitat de València, 1996, hep-ph/9703359 and ISBN:84-370-2989-9.
[25] M. Schmelling, MPI-H-V39-1996, Talk given at 28th Int. Conf. on High-energy Physics (ICHEP 96), Warsaw, Poland, July 1996, hep-ex/9701002.